# Infrared Sensing for Adaptive Arc Welding

*Infrared thermography is used to sense depth of penetration*

BY S. NAGARAJAN, W. H. CHEN AND B. A. CHIN

ABSTRACT. Adaptive welding enables dynamic altering of the welding parameters to compensate for changing environment. Sensors providing process status information in real time are an integral part of such an adaptive system. In this investigation, infrared thermography was used as a sensor to control the position of the arc and the penetration depth of the weld. Preliminary work on infrared thermography showed that variation in these parameters produces a change in the surface temperature distributions of the plates being welded. Subsequently, to achieve computer control of these variables, image analysis techniques have been developed to quantify the changes in the temperature distribution.

## Introduction

Adaptive welding is the key to success in the implementation of robotic welding systems. Quality of the weld produced by the robotic welding system depends primarily on accurate positioning of the weld pool and its depth of penetration. In a manual welding situation, the welder ensures the quality of the weld by monitoring and manipulating the process parameters according to the changing environment. The removal of the welder in the case of robotic welding has resulted in the loss of the ability to adapt to process fluctuations. Adaptive welding techniques attempt to emulate the functions of the replaced welder. Sensors provide the process status information of variables being controlled. Sensing techniques currently used in adaptive robotic welding systems mainly control a single variable such as joint tracking (Refs. 1–4). The joint tracking adaptive function has been investigated widely since it reduces the costs of high tolerance control in part preparation and fixturing. Infrared thermography has shown promise to detect the changes in several welding parameters by monitoring the surface temperature distributions of plates being welded (Ref. 5).

Preliminary investigations demonstrated that arc offset produced a definite asymmetry in the surface temperature distributions of the plates being welded (Ref. 5). In this work, image analysis techniques to quantify the asymmetry produced by arc offset have been identified. These quantitative relationships can then be used to joint track in real time. Weld joint penetration depth control is also a key function to be developed to produce reliable and consistent welds. There are two distinct cases of weld joint penetration control depending upon the thickness of the plates being welded. The first and simplest case is to maintain a fixed penetration depth in a plate of constant thickness (Refs. 6, 7). The second and more difficult case is to maintain a constant weld penetration depth in a plate with varying thickness. As a first step to achieve weld joint penetration control in plates with varying thickness, an approach is presented in this paper to identify the changes in the penetration depth of the plates being welded. The joint tracking work and the penetration control results are presented in two separate sections. Each section explains the approach used to analyze the various features of the thermal images and develop a quantitative relationship between the variations in the parameter studied and the corresponding changes in the thermal images.

## Joint Tracking

The schematic shown in Fig. 1 gives an overview of the experimental setup. The infrared camera, mounted on the welding gun assembly, monitors the temperature distribution around the weld pool. A custom-built interface transfers the information from the camera to the computer for analysis and feedback of appropriate corrective action.

## Experimental Procedure

All experiments were conducted using 6.35-mm (¼-in.) thick AISI 1040 steel plates 304.8 × 152.4 mm (12 × 6 in.) in size. The

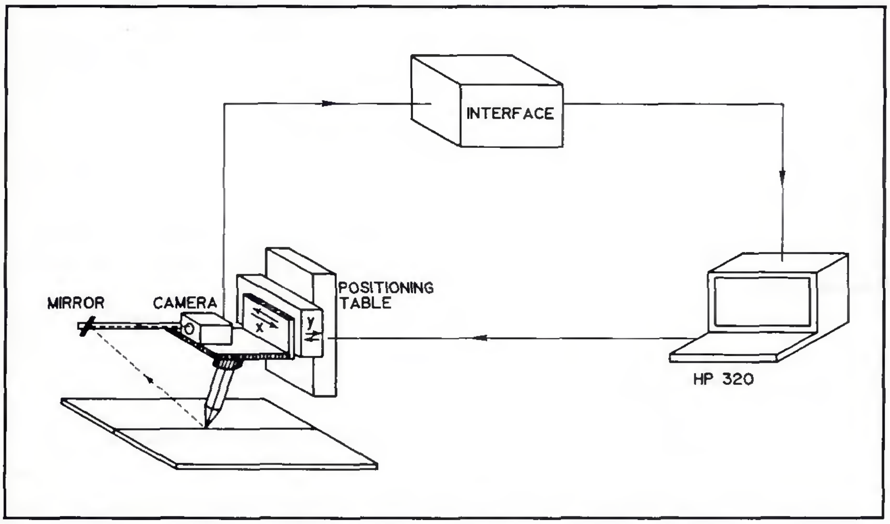


*Fig. 1 — Schematic of the experimental setup to demonstrate joint tracking*

**KEY WORDS**

Infrared Sensing
Adaptive Arc Welding
Infrared Thermography
Image Analysis
Temperature Distribution
Robotic Welding
Weld Pool Temp.
Joint Tracking
Penetration Variation
Penetration Control

*S. NAGARAJAN, W. H. CHEN and B. A. CHIN are with the Materials Engineering Department, Auburn University, Auburn, Ala.*

edges of the plates were milled to produce a precisely fitted butt joint. The surface of the plates was prepared using standard preparation techniques. Welding was performed with a Miller Synchrowave 500 AC/DC power source and a water-cooled torch. The torch was manipulated by an ESAB X-Y positioning table. This positioning table was controlled by a Hewlett Packard Series 320 computer through an HP 3497A data-acquisition/control unit. The infrared radiation that characterizes the thermal distribution of the plates being welded was detected by an Inframetrics Model 525 infrared camera. The infrared image from the camera was transferred to a Hewlett Packard Series 320 computer in a digital format and was also recorded on videotapes for future analysis. Each scan of the camera was transferred as a frame consisting of 192 × 250 discrete temperature measurements. The temperature distribution of plates being welded was represented as isotherms, regions of equivalent temperature. Two types of experiments were performed to derive the relationship between the arc offset and the asymmetry of the thermal profiles. The first type of experiment, parallel-joint experiment, was to weld along a straight line with a constant offset from the joint. In the second type of experiment, the cross-joint experiment, the experimental weld path was designed to start with a torch offset of 12.7 mm (½ in.) to the left of the joint and linearly across the joint to end with an offset 12.7 mm to the right of the seam. It is assumed that the effects of arc blow are negligible and the arc offset is caused only by torch offset. The weld conditions used in the experiments have been listed in Table 1.

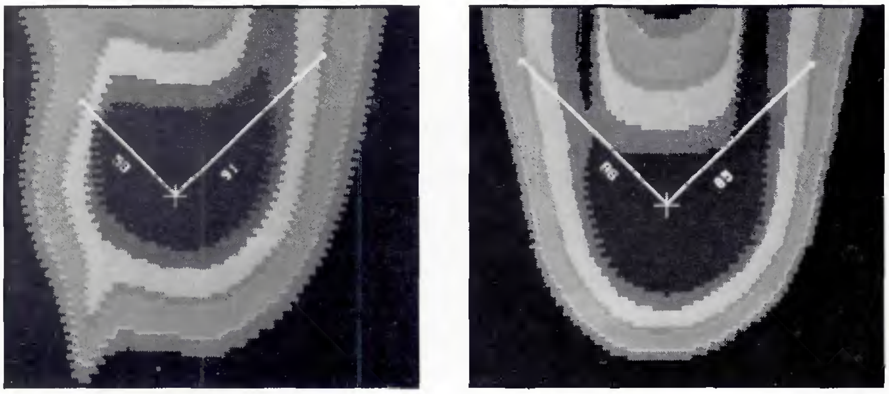

*Fig. 2 — Radii comparison technique to identify arc offset*

### Data Analysis

In order to identify the asymmetry, thermal profiles of on-joint and off-joint weld conditions were displayed as isotherms and visually compared. Figure 2 contains two isotherm patterns depicting the effect of arc offset on the thermal distribution of the plate. The thermal profiles obtained during on-joint welding conditions are illustrated by the pattern on the right, while the pattern on the left depicts the thermal profiles obtained during off-joint welding conditions. In on-joint welding conditions, the torch is placed over the center of the joint; and hence, the heat input to the plates by the welding gun is equally distributed on either side of the joint. This balanced thermal distribution yields isotherms that are symmetric about the center of the torch. In off-joint welding conditions, the torch is offset from the joint; and hence, the heat input is unequally distributed on either side of the joint. The unequal thermal distribution caused by the contact resistance of the joint is manifested in the asymmetry of thermal profiles. The contact resistance of the joint restricts the heat flow to the plate farther away from the torch, and hence reduces the maximum distance a single isotherm can reach in that plate. As the heat flow is unrestricted in the plate direction toward which the arc is offset, the maximum distance reached by any single isotherm is greater than the other plate. Thus, the asymmetry of isotherms is manifested in the size of the isotherms. The radius of an isotherm is a good measure of the size of an isotherm about the torch position. The radius of any isotherm is the distance between the calibrated torch position and the outer edge of the isotherm. Appropriately, the radius of an isotherm on the side toward which the torch is offset was found to be greater than the radius of the side farther away from the gun. For example, when the torch is offset to the left of the joint, it is expected that the left-hand-side radius should be greater than the right-hand-side radius. This would be true only if the welding process was monitored directly by the camera. But the process is monitored through a mirror and so the camera perceives only the mirror reflection of the images. Hence, the right radius is greater than the left — Fig. 2. In the figure, radii measurements along 45 deg in the direction opposite to the torch motion are superimposed on the isotherms. As the shape of the isotherms is different from that of a circle, the magnitude of the radii varies with the angle at which it is mea- sured. Radii along different angles were ana lyzed to identify the most responsive error signal. A comprehensive analysis revealed that the radii measurements along the welding gun row (0-deg direction), and 45 deg in a direction opposite to the motion of the torch yielded useful error signals.

This technique was used to analyze the parallel-joint and cross-joint experimental data. The error signals obtained are shown in Figs. 3 and 4. In both, the difference in radii is plotted along the y axes and the frame number along the x axes. The frame number is a function of time at which the frame of data was acquired. In the parallel-joint experiment, the frame number is inconsequential as the arc offset remains constant. However, the frame number is very useful in the cross-joint experiment, as the arc offset is a function of time. Therefore, the frame number is an indirect measure of the arc offset in a cross-joint experiment. In the parallel-joint experiment, as the arc offset is constant, the difference in radii remains a constant in the entire data file — Fig. 3. However, the magnitude of the difference in radii was found to vary with the direction of radii comparison. The magnitude of the error signal for 0-deg radii comparison is smaller than the error signal obtained through radii comparison along 45 deg against the direction of the torch. The radii comparison analysis of cross-joint data, yielded an error signal that starts with a negative difference in radii and linearly crosses the x axes, zero error, to terminate with a positive error magnitude — Fig. 4.

The absolute radii comparison error identification technique has its limitations. The magnitude of the error signal varies with plate thickness, penetration percentage and other variable weld parameters. For small penetration welds, the absolute magnitude of the error signal is very small. To avoid such variations, percentage difference instead of absolute difference in radii was investigated. Percentage difference in radii was computed as:

$$\text{percent difference in radii} = \frac{\text{difference in radii} \cdot 100}{\text{width of isotherm}/2} \qquad (1)$$

**Table 1—Welding Conditions**

| | |
|---|---|
| Welding gun speed | 2.7 mm/s (6.3 in/min) |
| Shielding gas | Argon, 18.87 L/min (40 $ft^3$/h) |
| Current | 200 A DC |
| Voltage | 20 V |
| Electrode | Negative EWTh-2, 0.3175 cm |

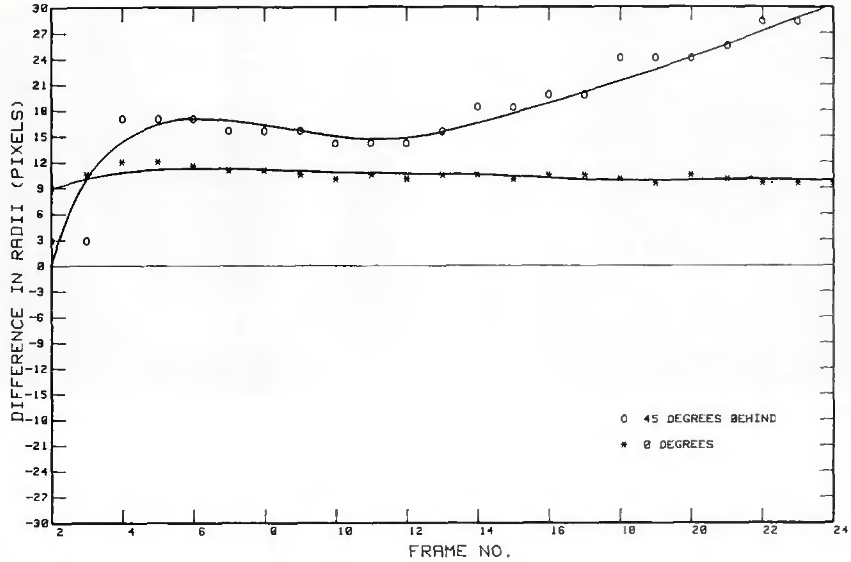


*Fig. 3 — Parallel-joint experiment radii comparison error signal*

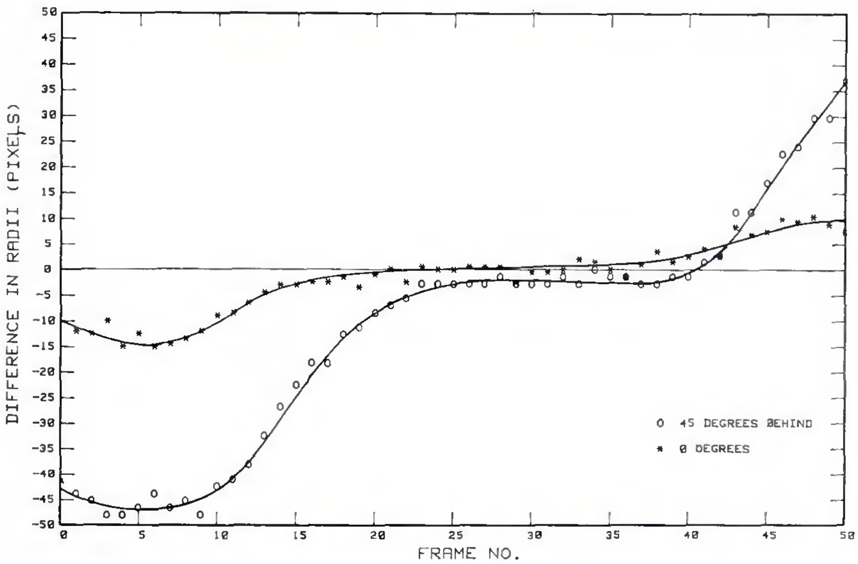


*Fig 4 — Cross-joint experiment radii comparison error signal*

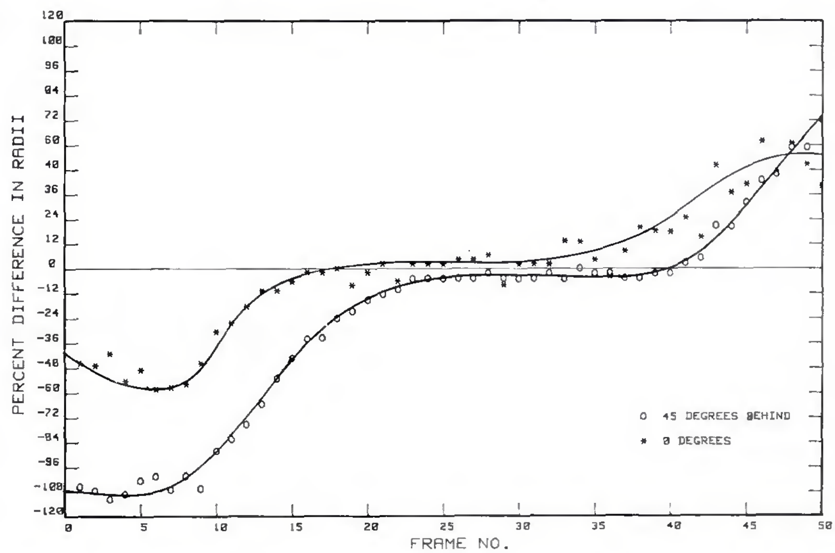


*Fig. 5 — Cross-joint experiment percent difference in radii error signal*

The cross-joint data was analyzed using the percent difference in radii technique. The magnitude of the error signal for the 0 deg radii comparison and 45 deg radii comparisons has improved tremendously — Fig. 5. The variations in the error signal were stabilized using a running average technique. In this technique, the average of the radii difference of the five preceding frames was computed. This computed average was then plotted on the y axes with the frame number along the x axes. This reduces the noise level in the error signal considerably — Fig. 6.

The results obtained from the analysis of the data through radii comparisons along different angles are unique. It has been proved that the arc offset can be detected by analyzing the thermal distributions. However, the time frame in which the sensor detects arc offset depends on the regions of the isotherms being analyzed to obtain the error signal. For instance, the radii comparison of the isotherm along the torch row (0 deg) provides information about the current status of the arc position with respect to the joint. Instantaneous arc position detection is possible in this case as the thermal distribution to the side of the torch is affected more drastically by the current location of arc. Analysis of the regions behind the torch would identify the previous torch position with respect to the joint. Therefore, the error signal obtained by comparing the radii along 45 deg in a direction opposite to the torch motion has a built-in time delay in detecting arc offset. In the data file presented, the torch crosses the joint at the 25th frame. This is determined using the time information recorded during data acquisition and the welding speed. As explained earlier, the instantaneous detection of arc position is possible with radii comparison along the 0 deg direction, and hence zero error occurs at the 25th frame of data. However, in the error signal obtained through radii comparison along 45 deg in the direction opposite to the motion of torch (Fig. 4), zero error occurs at a later frame. This delay in arc offset detection is a severe handicap during real-time joint tracking. Enhanced data acquisition and feedback response would minimize the disadvantage of deriving the error signal from the regions behind the torch.

## Penetration Variation Detection

Penetration variation detection experiments were conducted using the joint tracking experimental setup. The experimental weld path and the configuration of the plates used to perform the welds were different from the ones used for joint tracking experiments. Two distinct types of variations in the thickness of 304.8 × 152.4 mm (12 × 6 in.) plates were welded to monitor the effect of penetration depth variations on the isotherms. In one set of plates, the thickness was varied gradually from 6.35 mm (1/4 in.) to 3.175 mm (1/8 in.), but in the second set of plates, the changes were in steps of 1.587 mm (1/16 in.) for the same range of thickness variations. In both these plates, the experimental weld path was a straight bead on plate at the center of the plate.

### Data Analysis

The isotherm scheme was used to represent the thermal distribution of the plates being welded. The lower half of the isotherm represents the thermal distributions of the plate ahead of the weld pool. Hence, it is advantageous to be able to detect the variation of the depth of penetration by analyzing this half of the isotherm, as it provides additional time to compensate for the variation. The shape of the molten pool and the thermal distribution patterns associated with it are affected by the penetration depth of the weld. Therefore, the task of detecting the variation in the penetration depth would be simplified if one could identify a parameter that characterizes the changes in the shape of the molten metal pool and the associated thermal patterns. The isotherm, which represents the hottest regions of the plate being welded, best describes the changes in the molten pool. Hence, the changes in the features of this isotherm were monitored to understand the changes in the molten pool and thus identify variations in the penetration of the plate being welded.

A close scrutiny of the lower half of the interested isotherm revealed that its shape was close to an ellipse. Therefore, the outer edge of the isotherm was fitted using a least-squares method. This averaging technique yields a very good fit for the data and helps to minimize local variations in the isotherms due to welding process fluctuations. The analysis of the ellipse equation of the different frames of data obtained during the experimental weld run showed that two parameters of the ellipse, minor axes and the area of the ellipse changed with the penetration depth of the plate. As mentioned earlier, the changes in the size of the molten pool can be characterized by the changes in the size of the isotherm representing the hottest region of the plates. The analysis of the selected isotherm and its ellipse equation showed that the minor axes of the ellipse, and approximate measure of the size of the molten pool, was sensitive to the penetration depth of the plate. The area of the ellipse was also found to be sensitive to penetration depth changes as it is the integral of the width of the ellipse along the major axes. A plot of the change in penetration depth versus the corresponding change in the minor axes and the area of the ellipse for the two differ-

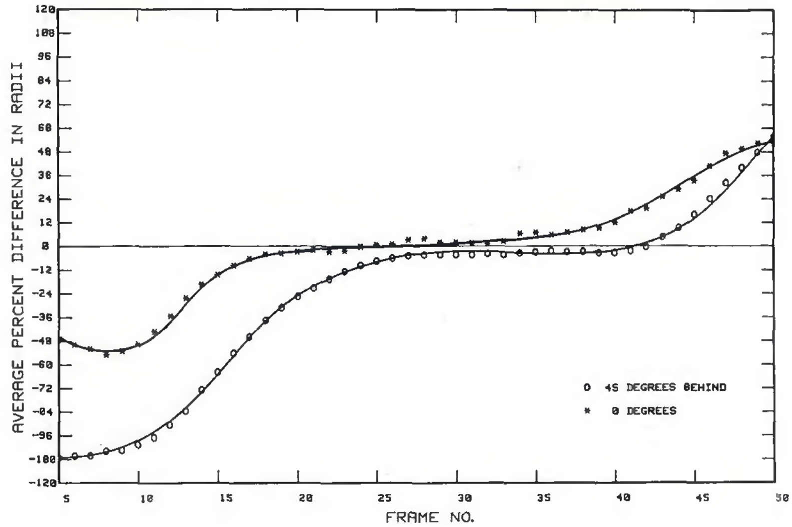


*Fig. 6 — Running average of percent difference in radii error signal*

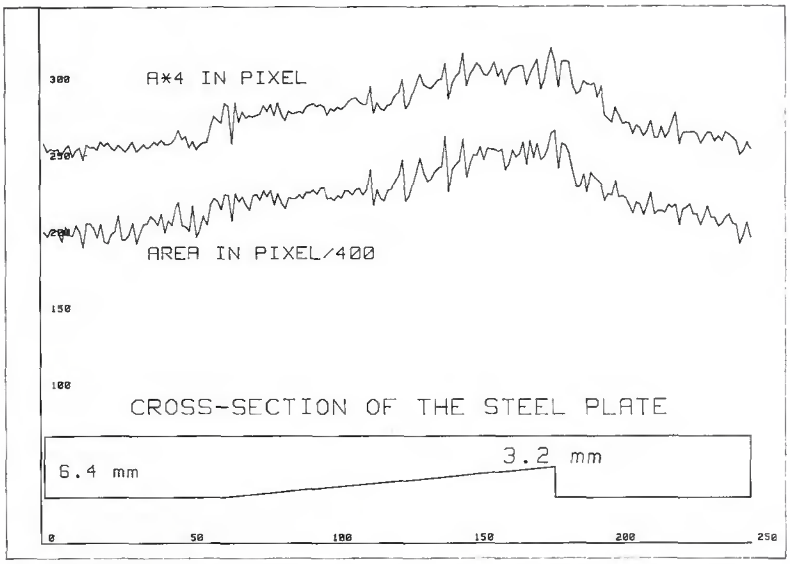


*Fig. 7 — Effect of penetration depth variation in a plate with gradual change in thickness*

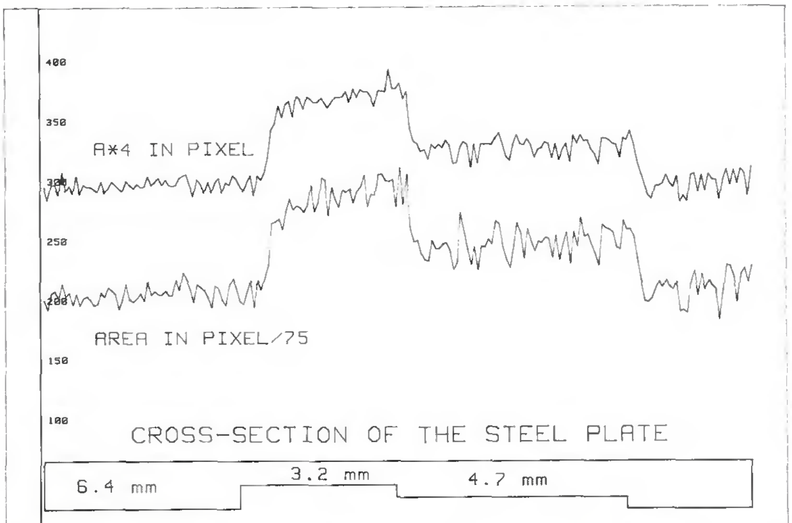


*Fig. 8 — Effect of joint penetration depth variation in a plate with step change in thickness*

ent types of experiments are shown in Figs. 7 and 8. The penetration depth changes that were detected in the experiments have a small time delay due to the heat transfer characteristics, both in the molten pool and the base metal. The delay time largely depends upon the torch speed, the thickness and the composition of the plates being welded.

## Conclusions

The following conclusions resulted from this investigation:

1) Isotherm radii can be used to identify arc position relative to the joint.

2) Comparison of the percent difference in radii instead of the absolute difference was found to improve the consistency of the obtained error signal.

3) Implementation of a running average for five data points was observed to reduce the noise level in the error signal.

4) The temperature distributions of the plates being welded change as joint penetration depth and thickness of the plates being welded change.

5) Minor axis and area of the ellipse of isotherms are the most sensitive variables to study changes due to the variations in the joint penetration depth and thickness of the plates being welded.

*References*


1. Cook, G. E. 1983. Through-the-arc sensing for arc welding. *Proceedings of 10th Conference on Production Research and Technology*, SAE, pp. 141–151.

2. Richardson, R. W. 1986. Robotic weld joint tracking systems — theory and implementation methods. *Welding Journal* 65(11):19–24.

3. Agapakis, J. E., Katz, J. M., Kolfman, M., Epstein, G. N., Friedman, J. M., Eyring, D. O., and Rutishauser, H. J. 1986. Joint tracking and adaptive robotic welding using vision sensing of the weld joint geometry. *Welding Journal* 65 (11):33–41.

4. Goldberg, F. 1985. Inductive seam tracking improves mechanized and robotic welding. *International Conference on Automation and Robotisation in Welding and Allied Processes*, pp. 393–400.

5. Chin, B. A., Madsen, N. H., and Goodling, J. S. 1983. Infrared thermography for sensing the arc welding process. *Welding Journal* 62(9):227-s to 234-s.

6. Wang, Y., and Chin, B. A. 1986. On-line sensing of weld penetration using infrared thermography. *Optical Techniques for Industrial Inspection* 665 (34):314–320.

7. Metcalfe, J. C. and Quigley, M. B. C. 1975. Automatic Control of Plasma Welding Using the Keyhole Efflux Plasma. *Welding Design and Metal Fabrication* 43 (11):674.